ANTICANCER RESEARCH *35*: 3341-3352 (2015)

# Characterization of Cells Cultured from Chylous Effusion from a Patient with Sporadic Lymphangioleiomyomatosis

IRMINA GRZEGOREK[1], EWA ZUBA-SURMA[2], MARIUSZ CHABOWSKI[3,4], DARIUSZ JANCZAK[3,4], ANDRZEJ SZUBA[5,6] and PIOTR DZIEGIEL[1]

*[1]Department of Histology and Embryology, and Departments of [4]Clinical Proceedings, and [6]Angiology, Faculty of Health Science, Wroclaw Medical University, Wroclaw, Poland;*
*[2]Department of Cell Biology, Faculty of Biochemistry, Biophysics and Biotechnology, Jagiellonian University, Krakow, Poland;*
*Departments of [3]Surgery and [5]Internal Medicine, Fourth Military Hospital, Wroclaw, Poland*

**Abstract.** *Background: Lymphangioleiomyomatosis (LAM) is a progressive, rare interstitial lung disease that almost exclusively affects women. It is caused by a mutation in one of the tuberous sclerosis genes, TSC1 or TSC2, and constitutive activation of the mammalian target of rapamycin (mTOR) pathway in smooth muscle-like cells (LAM cells). The heightened proliferation and accumulation of LAM cells leads to the destruction of lung tissue. Materials and Methods: In the present study, we developed a cell line (S-LAM1) derived from a chylous effusion obtained from a patient with sporadic, pulmonary LAM and evaluated its phenotype using immunofluorescence, flow cytometry, and an image stream system. Ultrastructure was assessed using a transmission electron microscope. To assess the ability of LAM cells to move and migrate (which is strictly associated with the ability to metastasize), we carried-out a real-time polymerase chain reaction (PCR) array analysis of 84 genes involved in cell motility. In order to evaluate the effect of rapamycin, a natural inhibitor of mTOR kinase, on S-LAM1 cells, a sulforhodamine B cell viability assay was performed with different concentrations of rapamycin. Results and Conclusion: The phenotype of these cells is consistent with the biology of LAM cells. S-LAM1 cells present combined smooth muscle, melanocytic, and lymphatic endothelium lineage, as well as the presence of mesenchymal differentiation markers. A particular pattern of gene expression, including high expression of ezrin (EZR), myosin heavy chain 10, non-muscle (MYH10), and myosin light chain kinase (MYLK) and a greatly decreased expression of supervillin (SVIL), when compared to controls, indicates a high potential motility activity, especially of cell spreading. Rapamycin significantly, although only partially, inhibited S-LAM1 cell proliferation in vitro, and should, perhaps, be considered in the future in combination with other agents.*

*Correspondence to:* Irmina Grzegorek, M.Sc., Department of Histology and Embryology, Wroclaw Medical University, Chalubińskiego 6a street, 50-368 Wroclaw, Poland. Tel: +48 717841365, Mobile: +48 501647494, Fax: +48 717840082, e-mail: irminagrzegorek@o2.pl

*Key Words:* Lymphangioleiomyomatosis, LAM cells, mTOR, rapamycin, cell motility, metastasis.

Lymphangioleiomyomatosis (LAM) is a progressive, rare interstitial lung disease that almost exclusively affects women. It is caused by a mutation in one of the tuberous sclerosis genes, *TSC1* or *TSC2*, leading to the constitutive activation of the mammalian target of rapamycin (mTOR) pathway and excessive proliferation of smooth muscle-like cells (LAM cells) (1). LAM may occur in a sporadic form (mutation of TSC gene in somatic cells), or may be associated with tuberous sclerosis complex (TSC), an autosomal-dominant disease characterized by hamartoma tumor formation in various organs, such as the skin, eyes, kidneys, lungs, and the central nervous system (2). LAM occurs in about 3 to 8 out of 1 million women and affects about 30% of women with TSC (1).

Intense proliferation and accumulation of LAM cells in the lungs and around the bronchi, blood, and lymphatic vessels leads to the destruction of the lung tissue and the formation of thin-walled cysts (3). LAM cell populations are heterogeneous and differ in morphology, localization in the LAM nodule, and marker expression. We can distinguish smaller, spindle-shaped, smooth muscle-like cells, which are located mostly in the central part of the LAM nodule, and larger epithelioid-like cells occurring peripherally (4, 5). The phenotype of LAM cells combines features of smooth muscle and melanoma cells. LAM cells express smooth muscle actin (αSMA), vimentin, and desmin, and are immunoreactive with human melanoma black 45 (HMB45), PNL2, and antibodies to CD63 (6). Immunohistochemical reaction with HMB45 has become a useful diagnostic tool in LAM (7).

LAM cells have the ability to be invasive and to metastasize; their presence has been observed in blood, urine, bronchoalveolar lavage fluid, and chyle (8-10). Metastasis and invasiveness is strictly dependent on cancer cell motility and migration. The mechanisms of cell motility include specific steps such as cytoskeletal reorganization, cell polarization, lamellipodial protrusion, adhesion, cell contractility, and detachment. Each step is regulated by a specific group of factors. Ras homolog gene family (RHO) proteins play an important role in these mechanisms. Moreover, many of the classic growth factors, such as epidermal growth factor (EGF) and hepatocyte growth factor (HGF), are known to promote cell migration (11, 12).

Excessive proliferation of LAM cells is caused by the constitutive activation of the mTOR pathway (1). To date, rapamycin (Sirolimus), a natural inhibitor of mTOR, seems to be the most promising therapeutic solution for LAM (13). Reductions in tumor volume and improvement in lung function has been reported in patients with LAM following treatment with rapamycin (14-16).

Sporadic LAM is an extremely rare disease; a useful experimental model of this disease is therefore necessary for further studies of its pathomechanisms. However, up-regulation of the mTOR pathway also occurs in many other types of neoplasm. The characterization and better understanding of LAM cell biology may facilitate research into new therapeutic approaches not only for LAM but also for other types of cancer.

In our study, based on this background, we characterized cells cultured from chylous effusion obtained from a patient with pulmonary, sporadic LAM. Phenotypic characterization of the derived S-LAM1 cells was performed using immunofluorescence, flow cytometry, and an image stream system. The ultrastructure of these cells was revealed by transmission electron microscopy (TEM). In order to gain insight into the cultured cell's ability to migrate, which is associated with the ability to metastasize, we performed a real-time polymerase chain reaction (PCR) array analysis of 84 genes involved in cell motility mechanisms. Finally, we investigated the influence of rapamycin on S-LAM1 cells using a sulforhodamine B (SRB) cell viability assay.

## Materials and Methods

*Cell culture*. S-LAM1 cells were cultured from the chylous effusion obtained from a 42-year-old female patient with sporadic pulmonary LAM. The case report has previously been presented (16). The cells were grown in Dulbecco's Modified Eagle's Medium (DMEM) (Lonza, Basel, Switzerland), containing 10% fetal bovine serum (Lonza) and 2 mM L-glutamine, at 37˚C in the presence of 5% $CO_2$. The cells were used in their fourth to tenth passages in all experiments.

Pulmonary artery smooth muscle cells (PASMs) (Lonza) were grown in smooth muscle growth medium-2 (SmGM-2) (Lonza) containing 5% fetal bovine serum at 37˚C in the presence of 5% $CO_2$. The cells were used in the fourth to eighth passages in all experiments. The study was approved by the Bioethical Committee of the Wrocław Medical University (approval number KB-594/2012).

*Fluorescence microscopy*. S-LAM1 cells grown on glass coverslips were incubated at 37˚C for 24 hours, and then washed with phosphate buffered saline (PBS). Cells were fixed in 4% glutaraldehyde for 10 min and washed with PBS. After washing, the cells were treated with 0.2% Triton-X and washed in PBS again. The slides were incubated at 4˚C overnight with primary antibodies: monoclonal mouse antihuman melanosome (clone HMB-45 at dilution 1:100; Dako, Glostrup, Denmark), monoclonal mouse antihuman α-SMA [clone 1A4, ready to use (RTU); Dako], monoclonal mouse antihuman vimentin (clone V9, RTU; Dako), and monoclonal mouse antihuman podoplanin (clone D2-40, RTU, Dako). After washing three times in PBS, the slides were incubated for 1 h at room temperature in the dark with donkey anti-mouse secondary antibody conjugated with fluorescein isothiocyanate (FITC) (Jackson ImmunoResearch Laboratories, Inc., West Grove, PA, USA), diluted 1:50 in antibody diluent (Dako). After washing, the slides were covered with Vectashield mounting medium for fluorescence with 4',6-diamidino-2-phenylindole (DAPI) (Vector Laboratories, Inc, Burlingame, CA, USA), and viewed and imaged with a BX51 fluorescence microscope (Olympus, Tokyo, Japan).

*Flow cytometry and image stream system*. For flow cytometric immunophenotyping, a single-cell suspension of S-LAM1 cells [in PBS with 2% fetal bovine serum (FBS) (Invitrogen, Carlsbad, CA, USA)] was stained with the following monoclonal antibodies against human antigens: CD45-FITC, hepatocyte growth factor receptor (c-MET-FITC), CD90-phycoerythrin (CD90-PE), CD105-PE, CD31-PE, CD29 PE-Cy5 (all antibodies from BD Bioscience, San Jose, CA, USA), STRO1-Alexa Fluor 647/APC (BioLegend, San Diego, CA, USA), CD133-allophycocyanin (CD133-APC) (Miltenyi Biotec, Bergisch Gladbach, Germany), HMB45-FITC (DAKO), and CD9-APC (BD Bioscience, San Jose, CA, USA). Cells were incubated with the directly conjugated antibodies for 30 min on ice and were subsequently washed and resuspended in PBS with 2% FBS for further multicolor analysis in an LSR II flow cytometer (Becton Dickinson, Franklin Lakes, New Jersey, USA).

Intracellular proteins, including vimentin and αSMA (DAKO), were identified in S-LAM1 cells following fixation [with 2% paraformaldehyde (Sigma, St. Louis, MO, USA) for 20 min at room temperature] and permabilization [with 0.2% Triton-X solution (Sigma) for 10 min at room temperature]. The washed cells were subsequently stained with anti-human vimentin or anti-human αSMA primary antibodies (mouse polyclonal IgG; Dako) and immunolabeled with antimouse secondary antibody conjugated with PE (BioLegend). All antibodies were added in accordance to the manufacturers' protocols. The cells were subsequently washed and resuspended in PBS with 2% FBS for further analysis in an LSR II flow cytometer (Becton Dickinson).

For immunophenotyping with imaging cytometry, S-LAM1 cells were stained as described above using the antibodies employed for classical flow cytometry (listed above). Cells were additionally stained with 7-aminoactinomycin D (7-AAD; according to the manufacturers' protocol) in order to visualize nuclei, and were subsequently analyzed using ImageStream X system (Amnis Corp., Seattle, WA, USA).

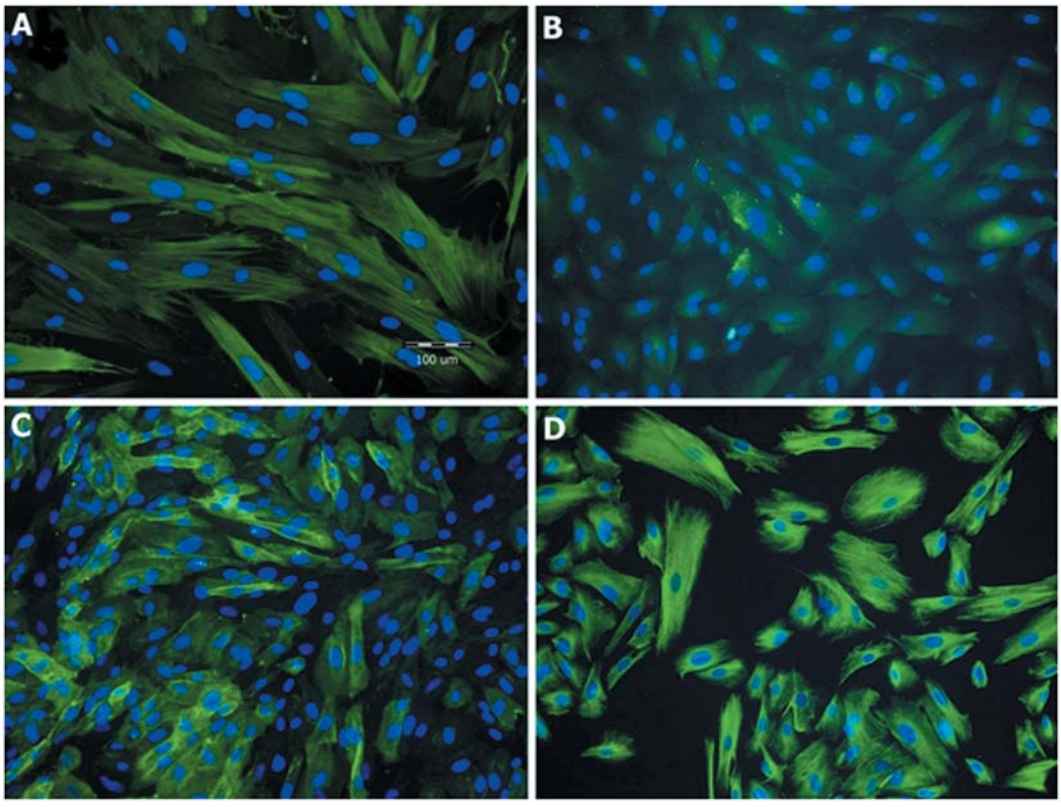


Figure 1. *Immunofluorescence characterization of S-LAM1 cells. Positive staining for α-smooth muscle actin (A), HMB-45 (B), podoplanin (C), and vimentin (D).*

*TEM*. In order to perform an ultrastructural analysis of the S-LAM1 cells, cells grown in 75 $cm^2$ flasks were trypsinized and fixed with 2.5% (v/v) glutaraldehyde (Merck, Dramstadt, Germany) in 0.1 M sodium cacodylate (Fluka, St. Gallen, Switzerland) at a pH of 7.4 for 30 min at room temperature. After washing in cacodylate buffer, the addition of bovine thrombin (Biomed, Lublin, Poland) and fibrinogen (Fluka) resulted in fibrin clot formation, in which the cells were entrapped. The samples were then postfixed with 2% (w/v) $OsO_4$ (Serva, Heidelberg, Germany) in 0.1 M cacodylate buffer for 1 h at RT, passed through a series of ethanol and acetone solutions, and finally embedded in Epon 812 (Roth, Karlsruhe, Germany). Ultrathin sections were prepared, stained with uranyl acetate/lead citrate (Fluka), and examined with a TEM JEM-1011 (JEOL, Tokyo, Japan).

*Human cell motility real-time PCR array*. Total RNA was extracted from six independent samples of S-LAM1 cells and PASMs using the RNeasy Mini Kit (Qiagen, Hilden, Germany) in line with the manufacturer's instructions. The RNA products were quantified by absorbance at 260 nm with a NanoDrop1000 spectrophotometer (NanoDrop Technologies, Wilmington, DE, USA). RNA quality was assessed using a bioanalyzer (Agilent, Santa Clara, CA, USA). First-strand cDNA was synthesized using the RT2 First Strand Kit (SABiosciences, Frederick, MD, USA). cDNA was subsequently combined with the RT2qPCR Master Mix, according to the manufacturer's instructions, and applied to pathway-specific RT2 Profiler PCR Arrays (SABiosciences, Frederick, MD, USA) for cell motility. This included a total of 96 genes involved in the movement of cells, such as growth factors and receptors important for chemotaxis, genes involved in RHO family signaling and adhesion, and genes encoding components of various cellular projections and control genes. A 7500 Real-Time PCR System (Applied Biosystems, Carlsbad, CA, USA) was used with the following cycle conditions: one cycle at 95 ˚C for 10 min, 40 cycles at 95 ˚C for 15 s, and 40 cycles at 60 ˚C for 1 min. During each annealing phase, SYBR green fluorescence was detected and recorded. The cycle threshold (Ct) values were recorded for each of the 96 wells, and expression levels were calculated using a standard equation for ΔΔCt. All expression levels were normalized to that of the housekeeping gene ribosomal protein L13 (*RPL13*), which did not vary significantly between PASM and S-LAM1 cells. The relative gene expression was examined by calculating the *n*-fold change in expression levels in the LAM cells, as compared with the PASMs. The *p*-values were calculated based on a Student's *t*-test of the replicate ΔΔCt values for each gene in the PASM and S-LAM1 cells, and *p*-values less than 0.05 were considered as statistically significant.

*Sulforhodamine B (SRB) cell viability assay*. S-LAM1 cells were plated at a density of 15,000 per well in 96-well format. The cells were grown for 24 h, reaching a confluence of 80%. Cells were treated with rapamycin (Sigma) at five different concentrations: 0.1 ng/ml, 1 ng/ml, 5 ng/ml, 10 ng/ml, 25 ng/ml, or control media, for 72 h. After

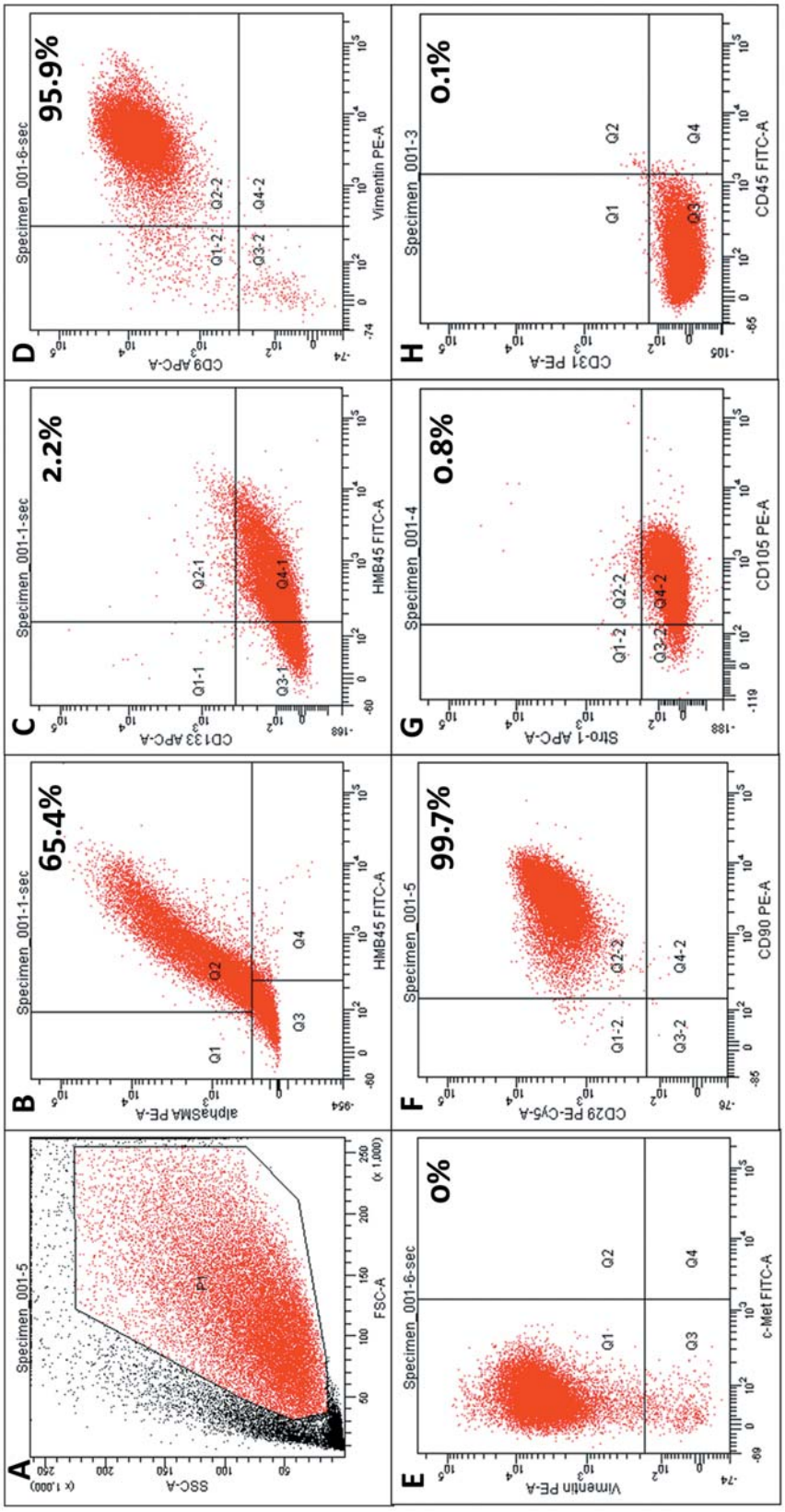


Figure 2. *Immunophenotyping of S-LAM1 cells by classical flow cytometry. A: Total population of S-LAM1 cells; B: co-expression of HMB-45 and α-smooth muscle actin (αSMA); C: HMB-45 and CD133; D: vimentin and CD9; E: c-MET and vimentin; F: CD90 and CD29; G: CD105 and stromal precursor antigen-1 (STRO1) H: CD45 and CD31 in S-LAM1 cells.*

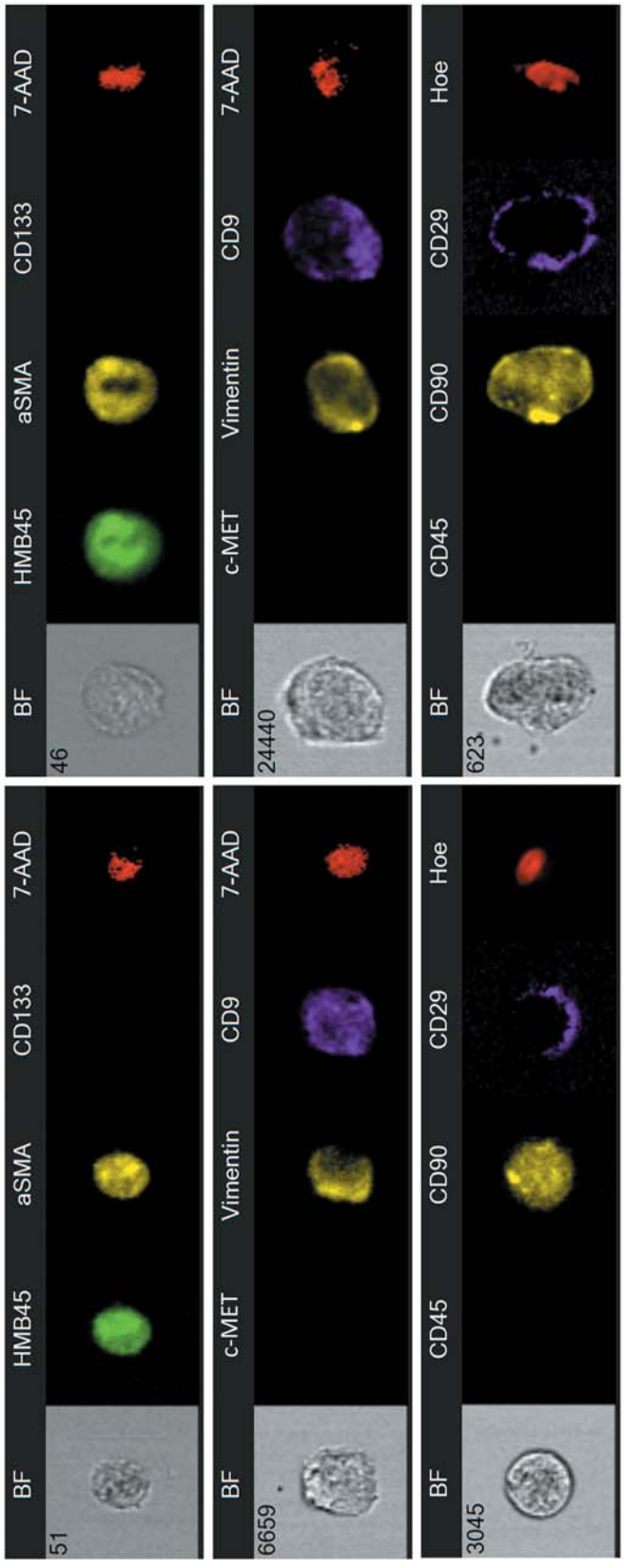


Figure 3. *Image Stream System characterization of S-LAM1 cells. A: Positive staining for HMB-45, α-smooth muscle actin (αSMA) and negative for CD133; B: negative staining for c-MET and positive for vimentin, CD9, C: negative staining for CD45 and positive for CD90 and CD29.*

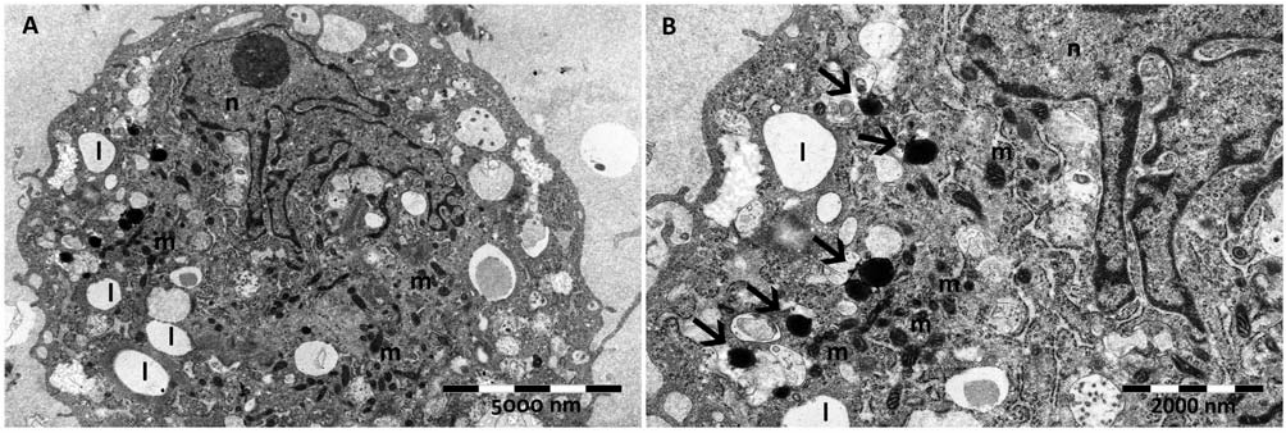


Figure 4. *Electron micrographs of S-LAM1 cell ultrastructure. A: Irregular surface of cell membrane due to the presence of cytoplasmic protrusions. Nucleus (n) is large, irregular and eccentrically located. Numerous tiny mitochondria (m) and lipid granules (l) are observed in cytoplasm. B: Cytoplasm of S-LAM1 cells contains electron-dense granules resembling immature melanosomes (arrows).*

treatment, 30 μl of trichloroacetic acid (TCA) solution (50% w/v in $H_2O$) per 100 μl medium was added to each well. The plates were incubated at 4˚C for 1 h for TCA cell fixation. Following fixation, the TCA solution was removed and the cell plates were washed five times with deionized water and allowed to dry at ambient temperature. Once the plates were completely dry, the cells were stained with SRB (0.4% in acetic acid, 50 μl/well) for 30 min at RT and than washed four times with 1% acetic acid in order to remove excess unbound dye. SRB was extracted from the dry, stained cells through the addition of 150 μl of Tris base (10 mM) and incubation for 30 min at RT. Absorbance was read at 564 nm on a universal microplate reader ELX800 (BIO-TEK Instruments, Inc., Winooski, VT, USA). The viability was expressed as a percentage that of the control treated with media. Student's t-test was used for the statistical analysis, *p*-values less than 0.05 were considered statistically significant.

## Results

*Phenotypic and ultrastructural characterization of the cultured cells*. We established a primary culture of S-LAM1 cells derived from the chylous effusion from a 42-year-old patient with pulmonary, sporadic LAM. The S-LAM1 cells were spindle-shaped. Immunofluorescence staining was conducted to characterize the S-LAM1 cells *in vitro*. Immunofluorescence staining exhibited significant αSMA (Figure 1A) and vimentin (Figure 1D) expression, that revealed the presence of intermediate actin and vimentin filaments. Staining with HMB-45 (Figure 1B), which is characteristic of melanoma cells, showed granular immunoreactivity with this antibody in the cytoplasm of cultured cells. Additionally, S-LAM1 cells exhibited strong-positive membrane expression of podoplanin (D2-40) (Figure 1C), a marker of lymphatic endothelial cells.

To further characterize the phenotype of the studied cells, flow cytometry was performed. Immunophenotypic analysis revealed that most cells exhibited co-expression of αSMA and

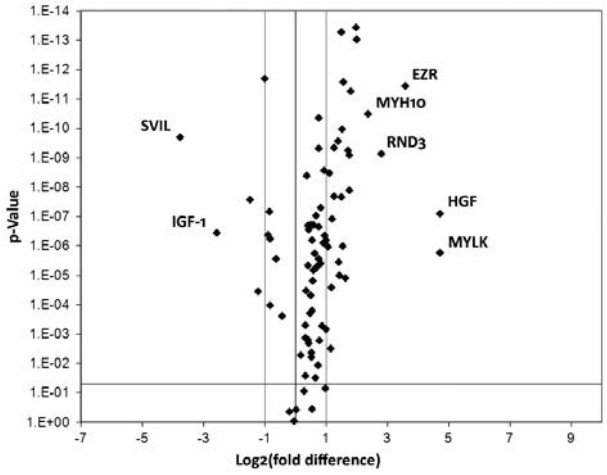


Figure 5. *Real-time polymerase chain reaction (PCR) 'cell motility' array, volcano plot. The vertical line in the middle of the plot indicates an n-fold change in gene expression of 1. The vertical lines on the left and on the right from the middle line indicate the desired n-fold change in gene expression threshold, defined as 2. The horizontal line indicates the desired threshold for the p-value of the t-test, defined as 0.05. The dots represent 84 genes involved in cell motility. Up-regulated genes in S-LAM1 cells are located in the upper-right square,while down-regulated genes are located in the upper-left square.*

HMB-45 (65,4%), vimentin and CD9 (95,9%), CD29 and CD90 (99,7%) and a lack of expression of CD45, CD31, CD133, STRO1, and c-MET (Figure 2). The expression of HMB-45, αSMA, vimentin, CD9, CD29, CD90, CD45, CD133, c-MET was further evaluated using an Image Stream System (flow-based imaging system). Co-expression of particular antigens in single LAM cells are presented in Figure 3.

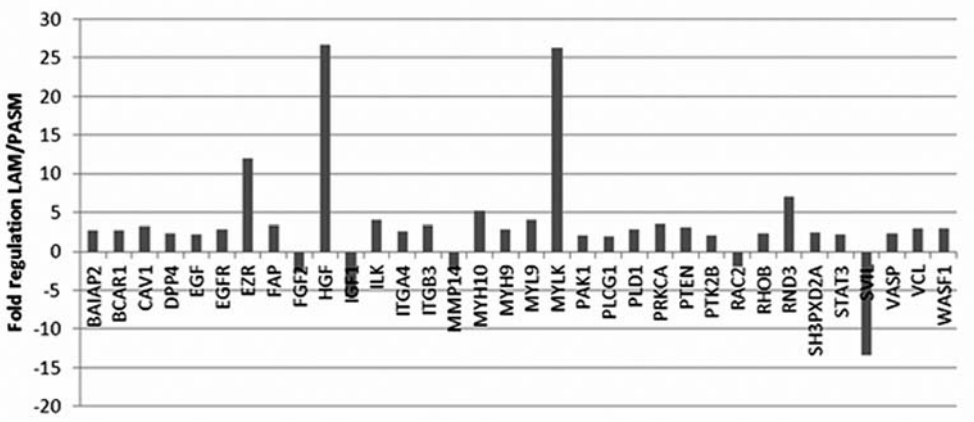


Figure 6. *Real-time polymerase chain reaction (PCR) 'cell motility'. A total of 34 out of 84 genes which entitled an at least two-fold and statistically significant change in expression in the S-LAM1 compared to PASMc cells ($p<0.05$).*

Ultrastructural analysis revealed that the S-LAM1 cells are covered with protrusions and microvilli, and have abnormal, irregular nuclei with a predominance of euchromatin over heterochromatin and containing 1-3 nucleoli. In the cytoplasm, numerous tiny mitochondria, lysosomes, some lipid granules, and expanded rough endoplasmic reticulum were observed, which indicate the intense metabolism typical of tumor cells. The presence of intermediate actin filaments and structures resembling pre-melanosomes supports the fact that LAM cells involve both the smooth muscle and melanoma lineages (Figure 4).

*Human cell motility PCR array.* To gain insight into the ability of S-LAM1 cells to metastasize, a real-time PCR analysis of 84 genes involved in cell motility was performed. The volcano plot in Figure 5 shows the relative change in gene expression between the tested samples (S-LAM1 cells) and the control cells (PASMc). A total of 34 genes exhibited at least a two-fold difference in the expression of all 84 cell motility genes in this array, with 29 genes being up-regulated and five genes being down-regulated in the LAM cultured cells; the *p*-value for the *t*-test was less than 0.05 (Figure 6). These genes are strictly associated with chemotaxis, adhesion, cellular projections, and membership of the RHO family of GTPases. The genes that were found to exhibit a more than fivefold change in expression are presented in Table I.

*Rapamycin inhibits LAM cell viability.* In order to study the effect of rapamycin on the proliferation of S-LAM1 cells, we employed five different doses of rapamycin: 0.1 ng/ml, 1 ng/ml, 5 ng/ml, 10 ng/ml, 25 ng/ml, and SRB. A cell viability assay was performed. The treatment of S-LAM1 cells with increasing doses of rapamycin resulted in a decrease in cell proliferation at doses of 1 ng/ml and higher ($p<0.05$). There were no statistically significant differences at doses lower than this. We observed 18%, 26%, 30%, and 34% inhibition of LAM cell viability following rapamycin treatment with doses of 1 ng/ml, 5 ng/ml, 10 ng/ml, and 25 ng/ml, respectively (Figure 7). There were no significant differences in cell viability between untreated cells (the control) and cells treated with the solvent control.

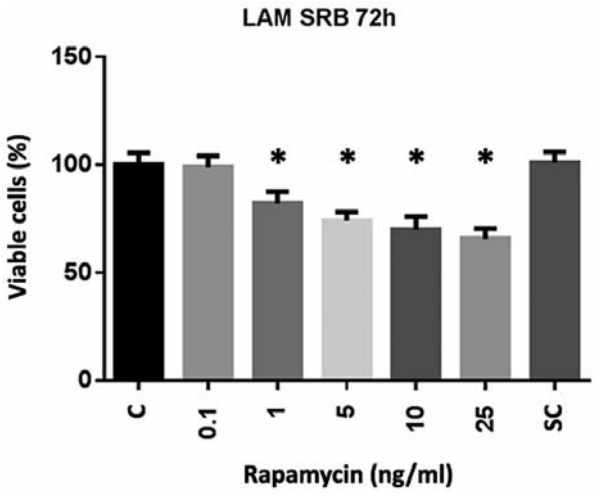


Figure 7. *Cell viability of rapamycin-treated S-LAM1 cells. *$p<0.05$ versus untreated cells (control). C, Control; SC, solvent control.*

## Discussion

LAM is a very rare interstitial lung disease. LAM cells are characterized by their excessive proliferation and ability to metastasize (4, 17). The phenotype of LAM cells combines the features of smooth muscle cells, lymphatic endothelial cells, and melanoma (18, 19). A mutation in one of the *TSC1* or *TSC2* genes results in the activation of mTOR kinase,

which is responsible for the regulation of growth, proliferation, and cell movement (17). The natural inhibitor of mTOR is rapamycin (4, 16). Although LAM occurs extremely rarely, dysregulation of the mTOR kinase pathway is involved in the pathogenesis of various human diseases, particularly cancer (*i.e.* breast cancer, lung cancer, melanoma, glioblastoma), hence the LAM cell line may be an interesting experimental model. The aim of our study was to phenotypically characterize cells cultured from chylous effusion obtained from a patient with sporadic, pulmonary LAM. In the next step, we evaluated the expression of 84 genes involved in cell motility. The effect of treatment with a natural inhibitor of mTOR kinase, rapamycin, on the viability of the S-LAM1 cells was also assessed.

The phenotypic evaluation of the S-LAM1 cell line using immunofluorescence staining showed the expression of αSMA, podoplanin (a marker of the lymphatic endothelium) and vimentin, as well as immunoreactivity with HMB-45 antibody, which reacts against an antigen present in melanocytic tumors, such as melanomas. Immunohistochemical staining with HMB-45 has become a useful diagnostic tool for LAM (7, 20). The combined smooth muscle and melanocytic differentiation in LAM was described in the study of Zhe *et al.* (6). The expression of melanocytic and smooth muscle markers in LAM cells has been extensively presented in the literature (18, 21, 22). The expression of vimentin, a type-III intermediate filament expressed mostly in mesenchymal cells, has been shown in proliferating spindle-shaped LAM cells in cases of pulmonary LAM (23, 24). The lymphatic endothelial differentiation of LAM (anti-podoplanin) cells is still controversial. The first immunohistochemical study using the D2-40 antibody reported no expression of podoplanin in LAM-like cells. Immunoreactivity with D2-40 has been shown in thin-wall lymphatic vessels accompanying LAM lesions (25). Contrary to these results, Davis *et al.* showed in their recent study positive immunohistochemical reaction of D2-40 in the majority of LAM cells in all the cases of sporadic LAM they investigated; there were no differences between early-stage and late-stage cases. Additionally, the expression of other lymphatic-specific markers, such as prospero homeobox protein 1 (PROX1), vascular endothelial growth factor receptor 3 (VEGFR3), and lymphatic vessel endothelial receptor 1 (LYVE1), was also shown in their study of LAM cells, which provides evidence that LAM cells in sporadic LAM may have an additional lineage of lymphatic endothelial differentiation (19). Our study supports these recent results.

Phenotypic evaluation of S-LAM1 cells by flow cytometry confirmed the expression of αSMA, HMB-45, and vimentin in these cells. Furthermore, we showed herein the expression of mesenchymal stem cell markers such as CD29, CD90, and CD105 in S-LAM1 cells. The origin of LAM cells remains unclear, but common features between migrating LAM cells and mesenchymal stem cells and cancer stem cells have been observed (2). It has been suggested that LAM cells may come from normal resident pulmonary vascular smooth muscle cells that undergo spontaneous somatic mutation, resulting in increased proliferation (17). Yan *et al.* described mesenchymal stem cell-like cells expressing the mesenchymal stem cells-specific surface proteins CD29, CD44, CD73, CD90 and CD105, which were derived from renal angiomyolipoma (26). These data suggest that one possible source of LAM cells in the lung could be the population of mesenchymal stem cells that have undergone spontaneous mutations and have differentiated into a migratory and proliferative phenotype. All S-LAM1 cells assessed by flow cytometry exhibited immunostaining with the antibody against CD9. CD9 is a cell surface glycoprotein that belongs to the tetraspanin family and is responsible for the modulation of adhesion, cell motility, and migration (27). The role of CD9 in many different types of carcinomas is variable. CD9 down-regulation correlates with increased cell motility and tumor progression in some types of carcinoma, such as breast, lung, and pancreatic carcinoma; other studies, however, show CD9 to be a cancer marker protein or an oncogene in ovarian carcinoma. Cancer such as head and neck squamous cell carcinoma, small-cell lung cancer and gastric cancer express higher levels of CD9 in their late stages (27, 28). As well as CD44v6, Cai *et al.* identified CD9 as a marker of disseminated cells with *TSC2* loss of heterozygosity in patients with LAM (10). Although we know that LAM cells express CD9, the role of this protein in LAM remains unclear. S-LAM1 cells did not show immunoreactivity with antibodies against CD45, CD31, c-MET, STRO1, or CD133. The expression of selected antigens assessed by flow cytometry was imaged using an Image Stream System, which shows the co-expression of these antigens in a single cell. The presence of intermediate actin filaments and electron-dense structures resembling pre-melanosomes, as seen in TEM, explains the immunoreactivity of the investigated S-LAM1 cells with antibodies characteristic of smooth muscle cell α-SMA and melanoma HMB-45. The cytoplasmic granules in LAM cells with electron-dense contents that show immunoreactivity with HMB-45 are considered immature melanosomes (stage I and II premelanosomes), and have been previously described (5, 18). The presence of protrusions and microvilli that cover the surface of the S-LAM1 cells reflects the motility of these cells. The phenotype of the S-LAM1 cell line presented in our study is consistent with the phenotypic features and biology of LAM cells.

The S-LAM1 cell line used in this study was derived from the chylous effusion of a patient with sporadic LAM, and we therefore expected this population to have the ability to move and migrate. The analysis of 84 genes involved in cell motility mechanisms in S-LAM1 cells, and the comparison with their expression in PASMc normal vascular smooth muscle cells, showed at least a two-fold change in the expression of 34 genes. Those genes that exhibited

Table I. *Real-time PCR 'cell motility' array: genes which showed at least a five-fold statistically significant change in expression in the S-LAM1 cells compared to PASMc ($p<0.05$), and their role in cell motility mechanisms.*

| Gene symbol | Name | Up/down-regulation multiplier | Role in cell motility |
|---|---|---|---|
| *EZR* | Ezrin | 12.01 | Cell–cell adhesion, cell polarity, cellular projections (filopodia, membrane blebs, invasive projections, membrane ruffles) |
| *HGF* | Hepatocyte growth factor | 26.61 | Growth factor, proteolysis |
| *IGF-1* | Insulin-like growth factor 1 | −5.85 | Growth factor |
| *MYH10* | Myosin, heavy chain 10, nonmuscle | 5.18 | Chemotaxis, cellular projections (stress fibers, membrane blebs) |
| *MYLK* | Myosin light chain kinase | 26.28 | RHO signaling, cellular projections (membrane blebs) |
| *RND3* | Rho family GTPase 3 | 7.01 | RHO signaling, cellular projections (membrane blebs) |
| *SVIL* | Supervillin | −13.40 | Cellular projections (filopodia, lamellipodia, invasive projections) |

altered expression were related to cell growth, chemotaxis, adhesion, RHO signaling, integrin-mediated signaling, cellular projections, cell polarity, and proteolysis. We identified seven genes whose expression was altered by at least a factor of five and may be involved in LAM pathophysiology: *EZR*; *HGF*; insulin-like growth (*IGF1*); myosin, heavy chain 10, nonmuscle (*MYH10*); myosin light chain kinase (*MYLK*); RHO family GTPase 3 (*RND3*), and supervillin (*SVIL*) (Table I).

Ezrin belongs to the ERM (ezrin-radixin-moesin) cytoskeleton-associated protein family and plays a crucial role in cell adhesion to the intracellular matrix, cell–cell interactions, receptor tyrosine-kinase signaling, RHO-GTPase signaling, and interactions with the protein kinase B (AKT)-mediated cellular apoptotic mechanisms; it is therefore thought to be involved in the cellular complexes and signaling pathways required for effective metastasis (29). It has been shown that ezrin plays an important role in the tumorigenicity and metastasis of lung cancer cells, and its silencing results in a reduction in cell migration and invasion; it also sensitized cancer cells to antitumor drugs (30). In pancreatic cancer cells, ezrin, by enhancing the formation of cell protrusions and cell microvilli and thus inducing ERK1/2 activation, has been shown to promote invasion and metastasis (31). Increased levels of ezrin in LAM cells, compared to normal vascular smooth muscle cells, may be associated with these cells' ability to migrate and metastasize. Wan *et al*. found a link between ezrin and mTOR signaling. The suppression of ezrin protein or the disruption of its function reduced lung metastasis in a mouse model, and also inhibited AKT phosphorylation and decreased the expression and phosphorylation of ribosomal protein S6 kinase (S6K1) and eukaryotic initiation factor 4E-binding protein 1 (4E-BP1), which are downstream targets of the mTOR pathway, in the K2M2 murine model of osteosarcoma (32). The role of ezrin in LAM cell metastatic behavior and its possible linkage with mTOR dysregulation in LAM is worth further evaluation.

Cell spreading is an early step in the complex cell motility process. Supervillin has been identified as a membrane-associated scaffolding protein that binds to MYH9, MYH10, MYLK, and actin filaments, and through this interaction inhibits cell spreading (33). It has been shown that a population of supervillin-transfected COS7 cells spreads less well than non-transfected cells on fibronectin and that the silencing of supervillin in A549 cells results in an increased rate of cell spreading (33). Myosin IIA and (especially) myosin IIB play an active role in promoting cell spreading (34), and thus cancer cell invasiveness (35). Myosin light-chain kinase, a calcium/calmodulin dependent enzyme, phosphorylates myosin regulatory light chains to facilitate myosin interaction with actin filaments, producing contractile activity. Inhibition of this kinase results in reduced cell spreading (34). The pattern of highly increased expression of MYH9, MYH10, and MYLK, accompanied by much decreased SVIL expression in S-LAM1 cells, as presented in our study, may be responsible for the promotion of LAM cell spreading, and thus of migration and metastasis.

RND3 is a protein involved in organization of the actin cytoskeleton and cell-cycle regulation, which has been described as a protein capable of inhibiting cell-cycle progression and inducing apoptosis in glioblastoma and prostate cancer cells (36). It has been shown that phosphorylation of 4E-BP1 is strongly suppressed in 3T3 RHOE-expressing cells and that RHOE may inhibit the 4E-BP1/eIF4E axis. Villalonga *et al*. suggest that it would be interesting to investigate whether there is a correlation between RHOE and eIF4E expression in tumors, and at the same time to assess the impact of RHOE as a modulator of the oncogenic function of eIF4E (37). *RND3* has been found to be up-regulated in subependymal giant cell astrocytomas, which are rare brain tumors associated with TSC (36). Similarly, we found *RND3* gene expression to be up-regulated in S-LAM1 cells compared to the control. The role of RND3 in LAM and in the mTOR pathway remains unclear, and needs to be further investigated.

Among growth factors, expression of HGF, which has been found to induce cancer cell motility (38, 39), increased greatly in S-LAM1 cells as compared to the PASMc normal vascular smooth muscle cells.

Rapamycin is a natural inhibitor of the mTOR signaling pathway and controls translation and cell proliferation. Rapamycin binds to the 12 kDa FK506 binding protein (FKBP12) cytosolic protein and inactivates mTOR kinase. Treatment with rapamycin results in a reduction in tumor volume and improved lung function in patients with LAM (15, 16). Treatment of S-LAM1 cells with increasing doses of rapamycin results in a decrease in cell proliferation at doses of 1 ng/ml and higher. It was reported by Lesma *et al*. that the treatment of *TSC2*$^{-/-}$ ASM cells, derived from an angiomyolipoma of a patients with TSC, with rapamycin at a dose of 1 ng/ml added at plating time was able to inhibit mTOR and the cell proliferation rate; however, the same dose added 3 h after plating did not affect cell proliferation (40). Interestingly, the higher doses of rapamycin (5 ng/ml, 10 ng/ml, 25 ng/ml) only slightly slowed S-LAM1 cell proliferation compared to rapamycin at a dose of 1 ng/ml. In the previously mentioned study, 10 ng/ml and 20 ng/ml concentrations of rapamycin, added 3 h after plating, also only slightly reduced *TSC2*$^{-/-}$ ASM cell proliferation. The influence of higher concentrations of rapamycin added at plating time on *TSC2*$^{-/-}$ ASM cell proliferation has not been shown (40). The hypothesis that rapamycin only partially inhibits cell growth, proliferation, and disease progression has been previously presented (41). It is possible that 1 ng/ml of rapamycin used *in vitro* is able to partially inhibit the proliferation of LAM cells, but the highly increased doses of rapamycin do not change this effect significantly. Using another agent that would synergize with rapamycin might perhaps inhibit further LAM cell proliferation, should be considered in the research into and treatment of LAM.

In summary, we developed a cell line derived from the chylous effusion from a patient with sporadic LAM. The phenotype of the cell line is consistent with the biology of LAM cells. S-LAM1 presents combined smooth muscle, melanocytic, and lymphatic lineage as well as the expression of mesenchymal markers, and can be considered a useful *in vitro* model of LAM. The particular pattern of gene expression, including the high expression of *EZR, MYH10*, and *MYLK*, and the much decreased expression of *SVIL* when compared to controls, indicate a high rate of motility activity, and especially of cell spreading. Rapamycin significantly but partially inhibits LAM cell proliferation *in vitro*, and should perhaps be considered in the future for use in combination with other agents.

## Acknowledgements

This study was supported by grant Pbmn84 from Wroclaw Medical University. The Authors express their appreciation to Dr Elzbieta Gebarowska, Dr Barbara Dolinska Krajewska and Dr Katarzyna Haczkiewicz for their collaboration and technical support.

## References

1 Henske EP and McCormack FX: LAM: a wolf in sheep's clothing. J Clin Invest *122*: 3807-3816, 2012.
2 Harari S, Torre O and Moss J: LAM: what do we know and what are we looking for? Eur Respir Rev *20*: 34-44, 2011.
3 Mavroudi M, Zarogoulidis P, Katsikogiannis N, Tsakiridis K, Huang H, Sakkas A, Kallianos A, Rapti A, Sarika E, Karapantzos I and Zarogoulidis K: LAM: current and future. J Thorac Dis *5*: 74-79, 2013.
4 Grzegorek I, Drozdz K, Podhorska-Okolow M, Szuba A and Dziegiel P: LAM cell biology and LAM. Folia Histochem Cytobiol *51*: 1-10, 2013.
5 Ferrans VJ, Yu ZX, Nelson WK, Valencia JC, Tatsuguchi A, Avila NA, Riemenschn W, Matsui K, Travis WD and Moss J: LAM (LAM): a review of clinical and morphological features. J Nippon Med Sch *67*: 311-329, 2000.
6 Zhe X and Schuger L: Combined smooth muscle and melanocytic differentiation in LAM. J Histochem Cytochem *52*: 1537-1542, 2004.
7 Bonetti F, Chiodera PL, Pea M, Martignoni G, Bosi F, Zamboni G and Mariuzzi GM: Transbronchial biopsy in lymphangiomyomatosis of the lung. HMB45 for diagnosis. Am J Surg Pathol *17*: 1092-1102, 1993.
8 Crooks DM, Pacheco-Rodriguez G, DeCastro RM, McCoy JP Jr., Wang JA, Kumaki F, Darling T and Moss J: Molecular and genetic analysis of disseminated neoplastic cells in LAM. Proc Natl Acad Sci USA *101*: 17462-17467, 2004.
9 Pacheco-Rodriguez G, Steagall WK, Crooks DM, Stevens LA, Hashimoto H, Li S, Wang JA, Darling TN and Moss J: *TSC2* loss in LAM cells correlated with expression of CD44v6, a molecular determinant of metastasis. Cancer Res *67*: 10573-10581, 2007.
10 Cai X, Pacheco-Rodriguez G, Fan QY, Haughey M, Samsel L, El-Chemaly S, Wu HP, McCoy JP, Steagall WK, Lin JP, Darling TN and Moss J: Phenotypic characterization of disseminated cells with TSC2 loss of heterozygosity in patients with LAM. Am J Respir Crit Care Med *182*: 1410-1418, 2010.
11 Wells A, Grahovac J, Wheeler S, Ma B and Lauffenburger D: Targeting tumor cell motility as a strategy against invasion and metastasis. Trends Pharmacol Sci *34*: 283-289, 2013.
12 Hanna S and El-Sibai M: Signaling networks of Rho GTPases in cell motility. Cell Signal *25*: 1955-1961, 2013.
13 Taveira-DaSilva AM and Moss J: Progress in the treatment of LAM: from bench to bedside. Rev Port Pneumol *18*: 142-144, 2012.
14 Davies DM, de Vries PJ, Johnson SR, McCartney DL, Cox JA, Serra AL, Watson PC, Howe CJ, Doyle T, Pointon K, Cross JJ, Tattersfield AE, Kingswood JC and Sampson JR: Sirolimus therapy for angiomyolipoma in tuberous sclerosis and sporadic LAM: a phase II trial. Clin Cancer Res 17: 4071–4081, 2011.
15 Bissler JJ, McCormack FX, Young LR, Elwing JM, Chuck G, Leonard JM, Schmithorst VJ, Laor T, Brody AS, Bean J, Salisbury S and Franz DN: Sirolimus for angiomyolipoma in tuberous sclerosis complex or LAM. N Engl J Med *358*: 140-151, 2008.
16 Chachaj A, Drozdz K, Chabowski M, Dziegiel P, Grzegorek I, Wojnar A, Jazwiec P and Szuba A: Chyloperitoneum, chylothorax and lower extremity lymphedema in woman with sporadic LAM successfully treated with sirolimus: a case report. Lymphology *45*: 53-57, 2012.

17 Finlay G: The LAM cell: What is it, where does it come from, and why does it grow? Am J Physiol Lung Cell Mol Physiol *286*: 690-693, 2004.
18 Matsumoto Y, Horiba K, Usuki J, Chu SC, Ferrans VJ and Moss J: Markers of cell proliferation and expression of melanosomal antigen in LAM. Am J Respir Cell Mol Biol *21*: 327-336, 1999.
19 Davis JM, Hyjek E, Husain AN, Shen L, Jones J and Schuger LA: Lymphatic endothelial differentiation in pulmonary LAM cells. J Histochem Cytochem *61*: 580-590, 2013.
20 Johnson S: Rare diseases. 1. LAM: clinical features, management and basic mechanisms. Thorax 54: 254-264, 1999.
21 Krymskaya VP: Smooth muscle-like cells in pulmonary LAM. Proc Am Thorac Soc *5*: 119-126, 2008.
22 Klarquist J, Barfuss A, Kandala S, Reust MJ, Braun RK, Hu J, Dilling DF, McKee MD, Boissy RE, Love RB, Nishimura MI and Le Poole IC: Melanoma-associated antigen expression in LAM renders tumor cells susceptible to cytotoxic T-cells. Am J Pathol *175*: 2463-2472, 2009.
23 Pan LH, Ito H, Kurose A, Yamauchi K, Inoue H and Sawai T: Pulmonary LAM: a case report with immunohistochemical details and DNA analysis. Tohoku J Exp Med *199*: 119-126, 2003.
24 Tawfik O, Austenfeld M and Persons D: Multicentric renal angiomyolipoma associated with pulmonary LAM: case report, with histologic, immunohistochemical, and DNA content analyses. Urology *48*: 476-480, 1996.
25 Hansen T, Katenkamp K, Bittinger F, Kirkpatrick CJ and Katenkamp D: D2-40 labeling in lymphangiomyoma/lymphangiomyomatosis of the soft tissue: further evidence of lymphangiogenic tumor histogenesis. Virchows Arch *450*: 449-453, 2007.
26 Yan X, Shi L, Chen G, Zhang X, Liu B, Yue W, Pei X and Sun S: Mesenchymal stem cell-like cells in classic renal angiomyolipoma. Oncol Lett *4*: 398-402, 2012.
27 Zöller M: Tetraspanins: push and pull in suppressing and promoting metastasis. Nat Rev Cancer *9*: 40-55, 2009.
28 Hwang JR, Jo K, Lee Y, Sung BJ, Park YW and Lee JH: Upregulation of CD9 in ovarian cancer is related to the induction of TNFα gene expression and constitutive NFκB activation. Carcinogenesis *33*: 77-83, 2012.
29 Hunter KW: Ezrin, a key component in tumor metastasis. Trends Mol Med *10*: 201-204, 2004.
30 Chen QY, Xu W, Jiao DM, Wu LJ, Song J, Yan J and Shi JG: Silence of ezrin modifies migration and actin cytoskeleton rearrangements and enhances chemosensitivity of lung cancer cells *in vitro*. Mol Cell Biochem *377*: 207-218, 2013.
31 Meng Y, Lu Z, Yu S, Zhang Q, Ma Y and Chen J: Ezrin promotes invasion and metastasis of pancreatic cancer cells. J Transl Med *8*: 61, 2010.
32 Wan X, Mendoza A, Khanna C and Helman LJ: Rapamycin inhibits ezrin-mediated metastatic behavior in a murine model of osteosarcoma. Cancer Res *65*: 2406-2411, 2005.
33 Takizawa N, Ikebe R, Ikebe M and Luna EJ: Supervillin slows cell spreading by facilitating myosin II activation at the cell periphery. J Cell Sci *120*: 3792-3803, 2007.
34 Betapudi V, Licate LS and Egelhoff TT: Distinct roles of nonmuscle myosin II isoforms in the regulation of MDA-MB-231 breast cancer cell spreading and migration. Cancer Res 2006 *66*: 4725-4733, 2006.
35 Duxbury MS, Ashley SW and Whang EE: Inhibition of pancreatic adenocarcinoma cellular invasiveness by blebbistatin: a novel myosin II inhibitor. Biochem Biophys Res Commun *313*: 992-997, 2004.
36 Tyburczy ME, Kotulska K, Pokarowski P, Mieczkowski J, Kucharska J, Grajkowska W, Roszkowski M, Jozwiak S and Kaminska B: Novel proteins regulated by mTOR in subependymal giant cell astrocytomas of patients with tuberous sclerosis complex and new therapeutic implications. Am J Pathol *176*: 1878-1890, 2010.
37 Villalonga P, Fernández de Mattos S and Ridley AJ: RhoE inhibits 4E-BP1 phosphorylation and eIF4E function impairing cap-dependent translation. J Biol Chem *284*: 35287-35296, 2009.
38 Radtke S, Milanovic M, Rossé C, De Rycker M, Lachmann S, Hibbert A, Kermorgant S, Parker PJ: ERK2 but not ERK1 mediates HGF-induced motility in non-small cell lung carcinoma cell lines. J Cell Sci *126*: 2381-2391, 2013.
39 Rø TB, Holien T, Fagerli UM, Hov H, Misund K, Waage A, Sundan A, Holt RU and Børset M: HGF and IGF1 synergize with SDF1α in promoting migration of myeloma cells by cooperative activation of p21-activated kinase. Exp Hematol *41*: 646-655, 2013.
40 Lesma E, Grande V, Ancona S, Carelli S, Di Giulio AM and Gorio A: Anti-EGFR antibody efficiently and specifically inhibits human *TSC2*$^{-/-}$ smooth muscle cell proliferation. Possible treatment options for TSC and LAM. PLoS One *3*: e3558, 2008.
41 Yu J, Parkhitko AA and Henske EP: Mammalian target of rapamycin signaling and autophagy: roles in LAM therapy. Proc Am Thorac Soc *7*: 48-53, 2010.

*Received March 11, 2015*
*Revised March 24, 2015*
*Accepted March 27, 2015*